EGTRIB Journal
JOURNAL OF
THE EGYPTIAN SOCIETY OF TRIBOLOGY
VOLUME 19, No. 4, October 2022, pp. 63 - 74 **ISSN 2090 - 5882**
(Received July 25. 2022, Accepted in final form August 18. 2022) **jest.journals.ekb.eg**

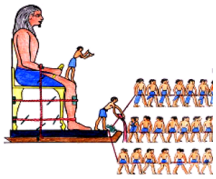

CONTACT AND SEPARATION OF KAPTON AND POLYMETHYLMETHACRYLATE TRIBOELECTRIC NANOGENERATOR

Al-Kabbany A. M. and Ali W. Y.

Faculty of Engineering, Minia University, P. N. 61111, El-Minia, EGYPT.

ABSTRACT

Triboelectric nanogenerators are devices that utilize the triboelectric effect in order to generate electrical current. Recently, they have become very popular in many applications. The most important are self-powered sensors and energy harvesting. They can be made in two varieties, contact-and-separation mode as well as sliding mode triboelectric nanogenerator (TENG). Two of the best pair of materials that can be used are Kapton and polymethylmethacrylate (PMMA) since they are at opposite sides of the triboelectric series. Usually, the entire side of a TENG is covered with a dielectric electrode terminal. This study investigates the optimal design of a Kapton side in a Kapton/PMMA contact and separation mode triboelectric nanogenerator.

It was found that using two Kapton-electrode terminals that are separated by a distance achieved better values for both open-circuit voltage and closed-circuit current in this particular setup. This is due to the self-correcting mechanism that is inherent in this setup that improves the contact between the two sides of the triboelectric nanogenerator. This design is also more material efficient and is thus recommended for use in contact and separation mode triboelectric nanogenerators.

KEYWORDS

Kapton, polymethylmethacrylate, contact and separation, triboelectric nanogenerator.

INTRODUCTION

If two materials are forced to contact each other, there is a high likelihood that charges are pumped from one material to the other. This is known as triboelectrification, [1 - 4]. Triboelectrification is one of the oldest physical phenomena ever observed. It is still not well-understood. In metals, it is highly likely that triboelectrification occurs due to differences in the work function of two metals, however, in dielectric materials, the mechanism is still not clear, with ion transfer being a likely explanation, [5].

Predicting the intensity and sign of the induced charges on each surface due to the triboelectric effect is done using the triboelectric effect, [6 - 8]. It is a series that may rank materials by the likelihood of induction of a positive charge on the surface of the material. Kapton has a high likelihood of obtaining a negative charge upon contact with another material, [9], while PMMA is one of the materials which are located near the top of the triboelectric series and is thus likely to obtain a positive charge, [10]. So, if Kapton and PMMA come into contact with one another, Kapton will gain a high value of negative charge, while PMMA will gain a high value of positive charge.
The TENG is made of two dielectric materials which are on opposite sides of the triboelectric series connected to electrodes. When the two dielectric surfaces come into contact with each other, they induce equal and opposite charges on each surface. This potential difference is used in order to produce an electric current. It has two main uses, as energy harvesters, [11-14], and as self-powered sensor, [15 - 18]. The output open circuit voltage of a TENG can be predicted using the V-Q-x equation, [19], but other TENG characteristics can be predicted using other models, [20 - 21]. It is also known that as the contact force pressing the two sides of a TENG increases, the output voltage tends also to increase, [21].

TENGs can be classified into contact and separation mode TENGs, [22 - 23] and sliding mode TENGs, [24 - 25]. In contact and separation mode TENGs, the two dielectrics are usually separated by an elastic spacer such as a spring or a sponge that separates the dielectrics once the dielectrics come into contact. However, if all the surface of each one of the sides of the TENG was fully covered by a dielectric-electrode terminal, this would increase the price of production of a certain TENG.

This study investigates the optimal design of the Kapton side of a Kapton/PMMA contact and separation mode TENG based on both performance and cost.

EXPERIMENTAL

In this experiment, three different setups of a Kapton/PMMA TENG were tested, the first side of the TENG was made of a 500 mm by 500 mm wooden plate, attached to 400 mm by 400 mm slate of 2.5 mm thick PMMA coated on one side with aluminum foil, for the Kapton side. The setup was composed of various terminals arranged in different configurations, a Kapton terminal is 100 mm by 100 mm made of three layers, a layer of 320 grit sandpaper, a layer of aluminum foil setup above it, and a layer of Kapton above it. The first setup was composed of three of these terminals arranged side by side and were connected in series with 10 mm distance and placed on a 5 mm thick support structure then they were put in the middle of a 500 mm by 500 mm wooden plate as shown in Fig. 2. The second setup was composed of six Kapton terminals, each three of them was put on a support and the distance between the two supports was 100 mm, Fig. 3. All the terminals were also connected in series. The third setup was composed of nine terminals with three supports, each support with three terminals, where the supports were right next to one another and all the terminals were connected in series, Fig. 4.

The two sides of the TENG were separated with four sponges, so that the distance between the surface of the PMMA side and the surface of the Kapton side is 15 mm. Two operators of 750 and 1200 N weight both stepped on the TENG and then stepped off, with the open

circuit voltage between both sides being measured upon the operator stepping on and stepping off the TENG being recorded. The experiment was also repeated for each weight to measure the short circuit current.

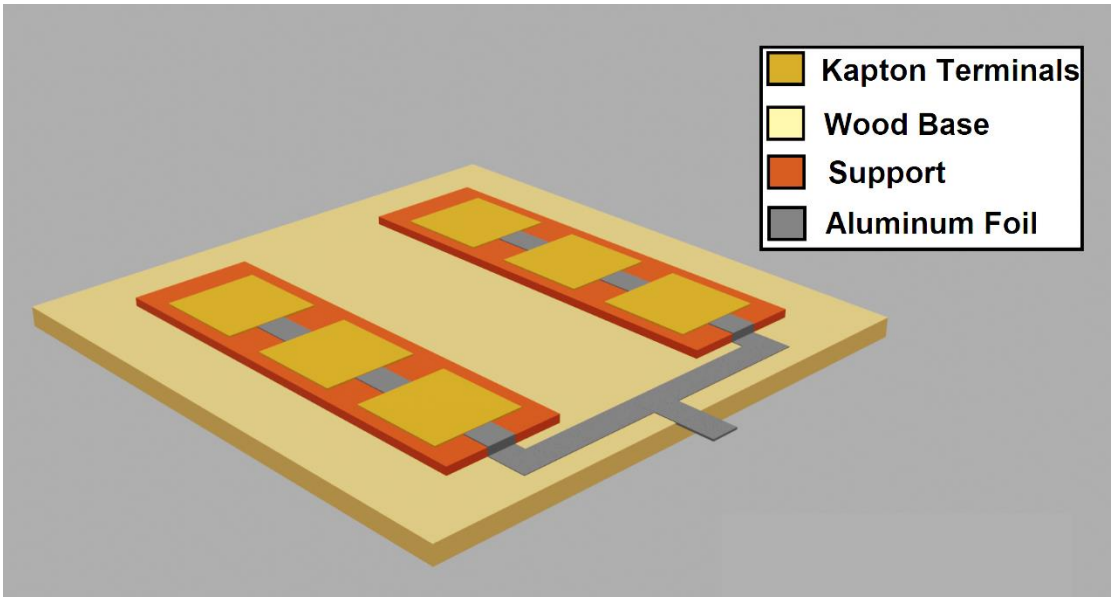

Fig. 1 Components of the Kapton side of the TENG.

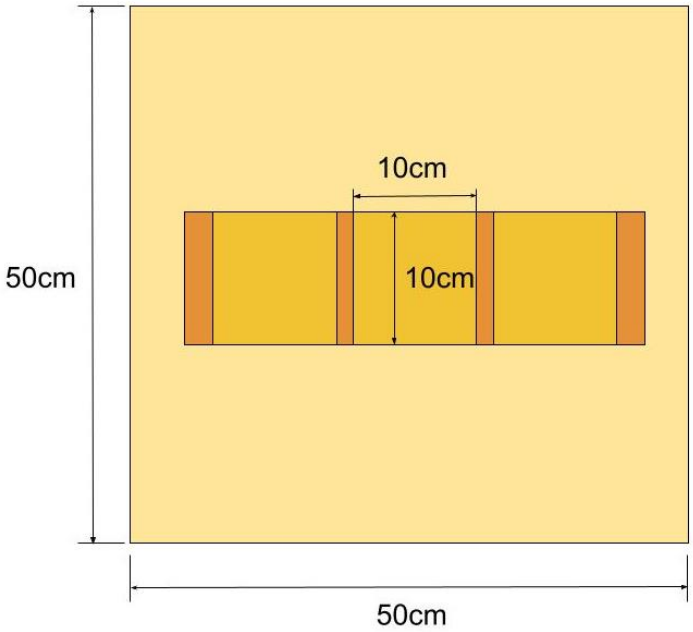

Fig. 2 First setup.

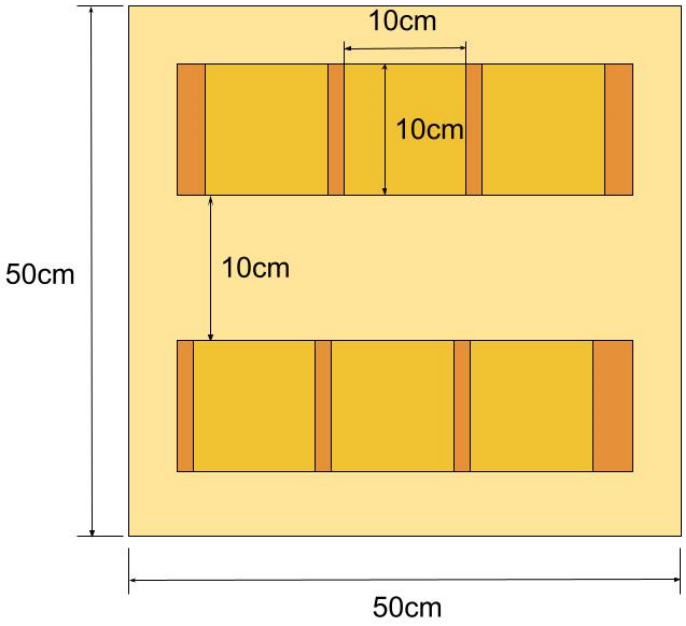

Fig. 3 Second setup.

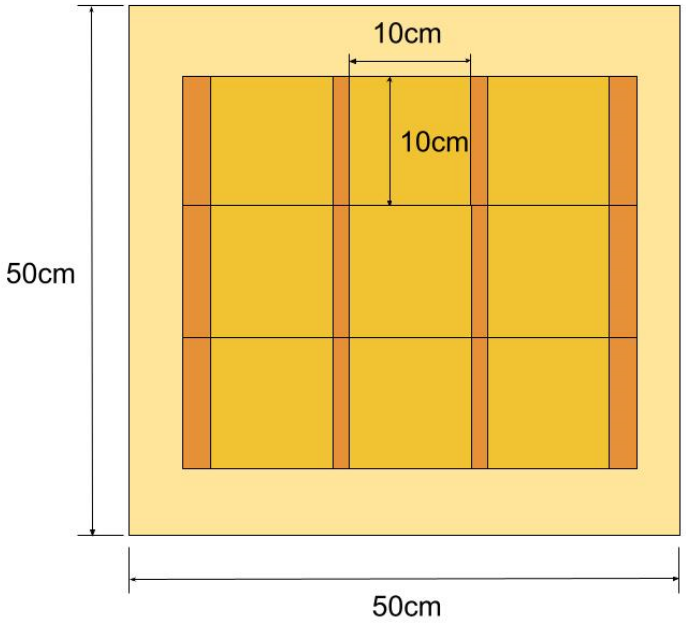

Fig. 4 Third setup.

Fig. 5 The Proposed TENG.

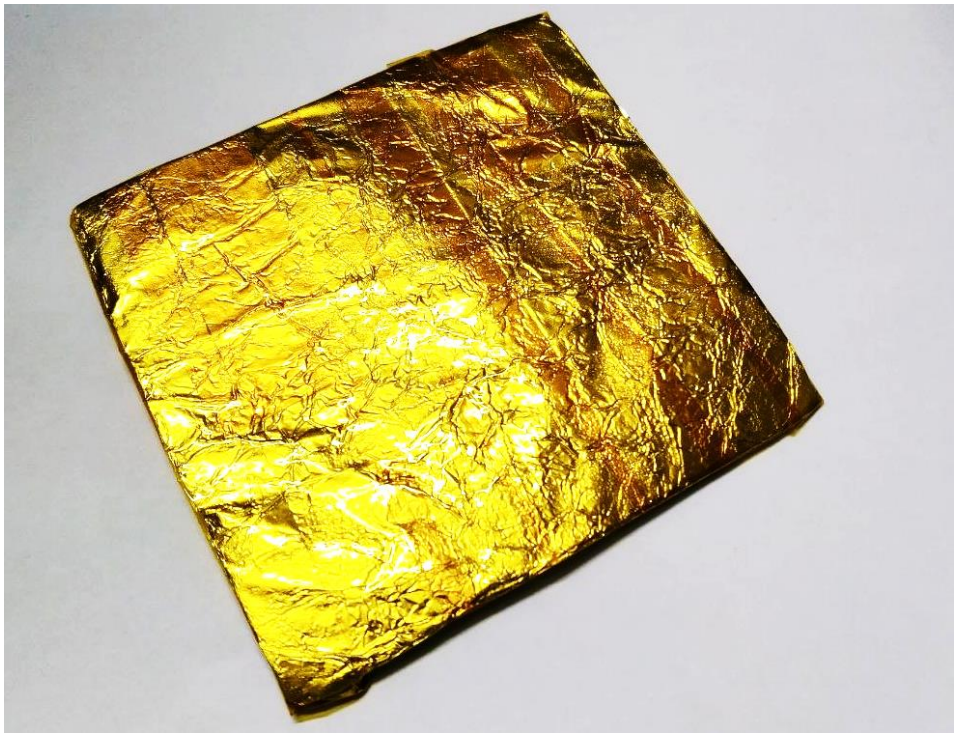

Fig.6, One of the 100 mm by 100 mm Kapton terminals.

RESULTS AND DISCUSSION

The results of this experiment are reported in Figs. 7 to 12.

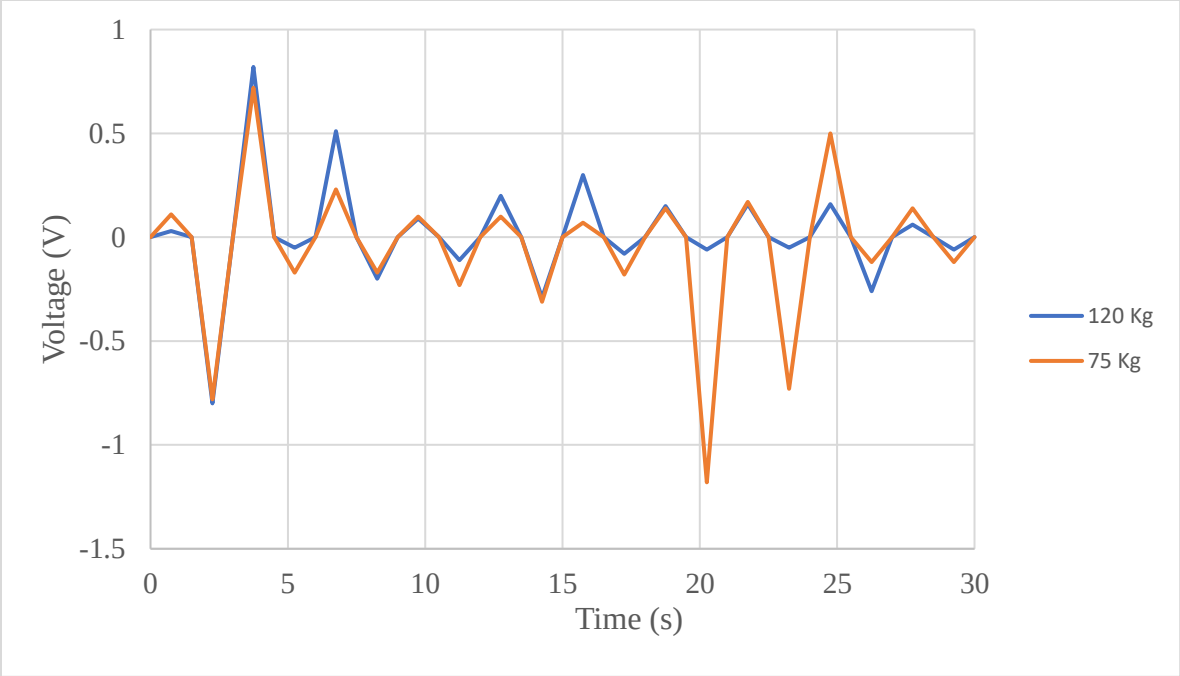

Fig. 7 Voltage (in Volts) in the first setup.

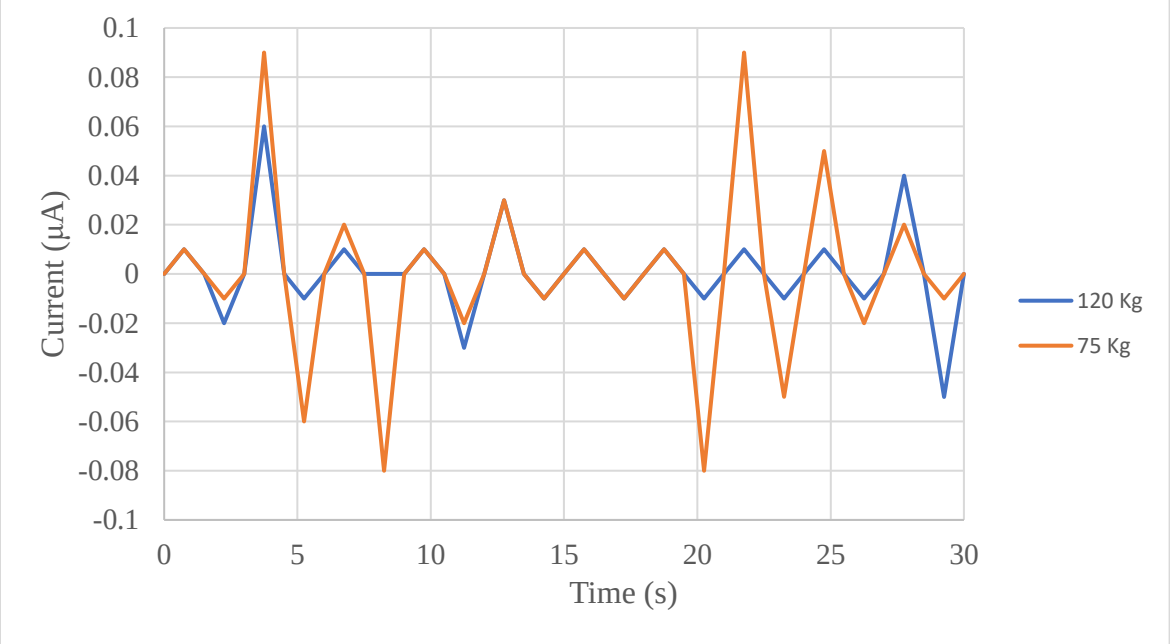

Fig. 8 Current (in Micro Amperes) in the first setup.

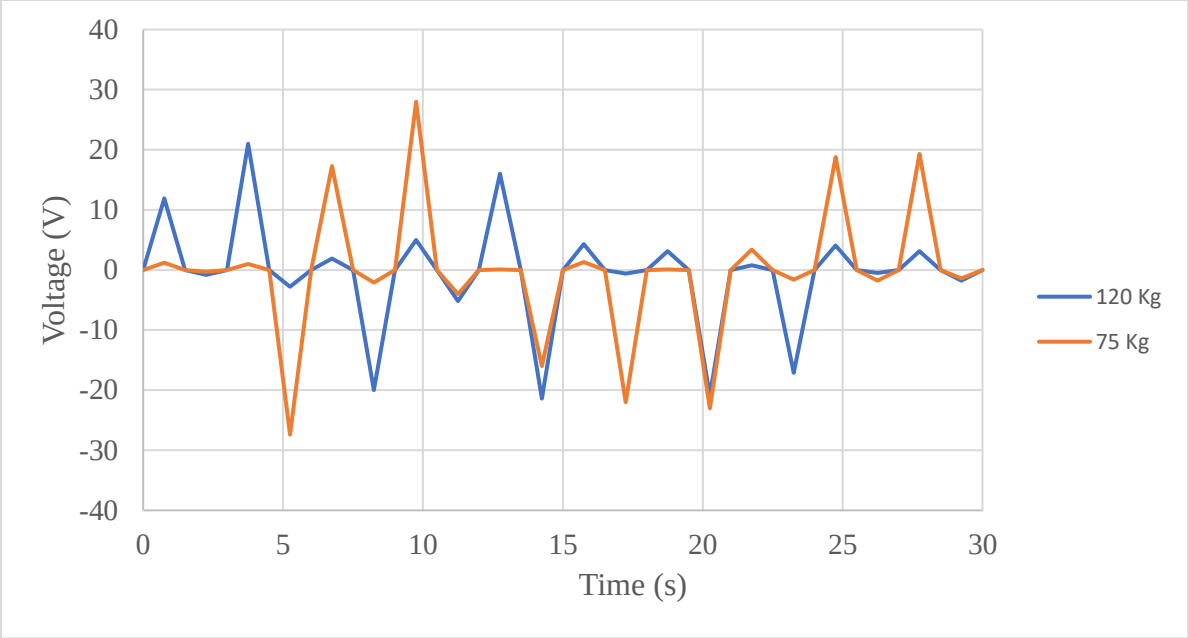

Fig. 9 Voltage (in Volts) in the second setup.

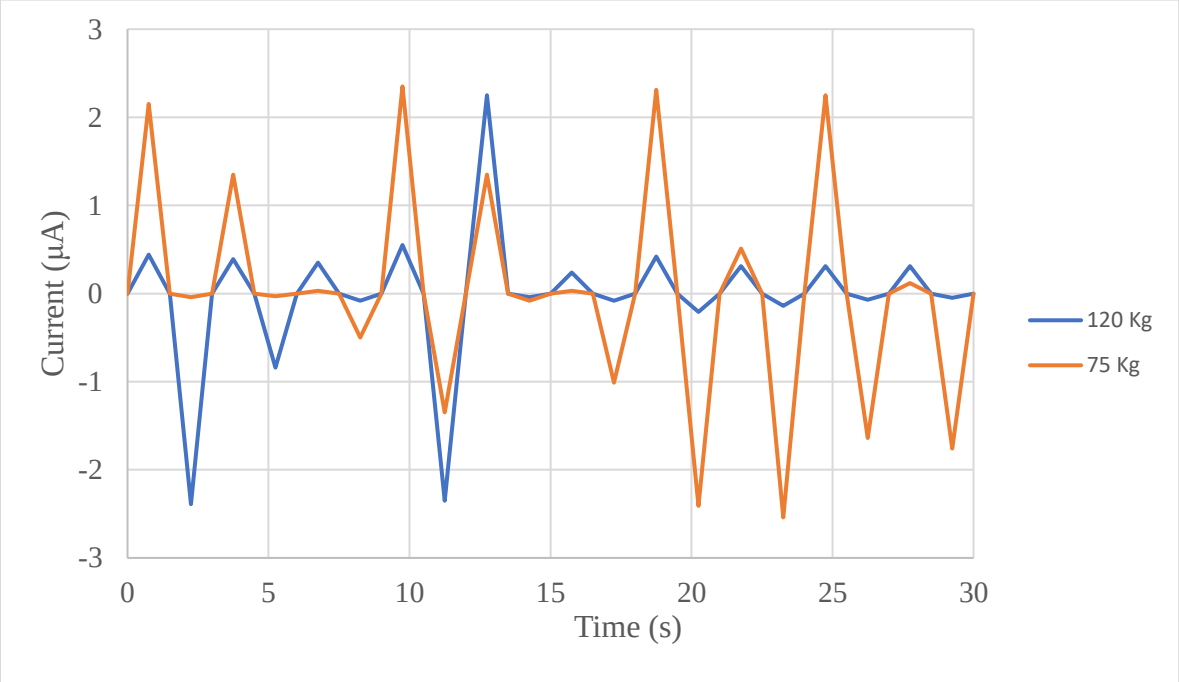

Fig. 10 Current (in µA) in the second setup.

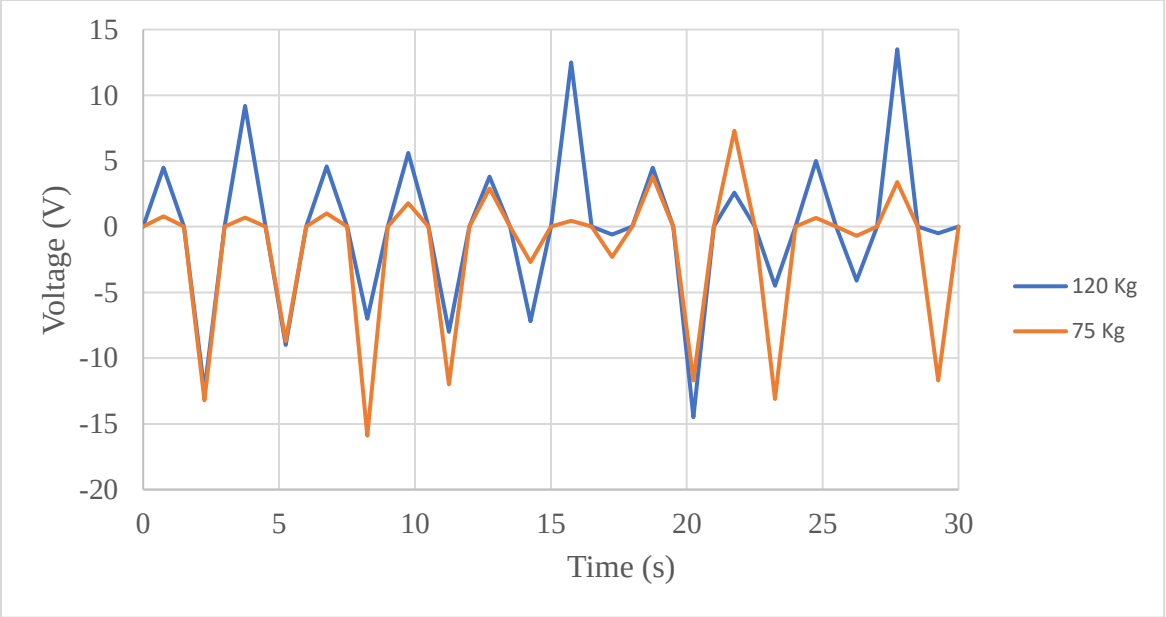

Fig. 11 Voltage (in Volts) in the third setup.

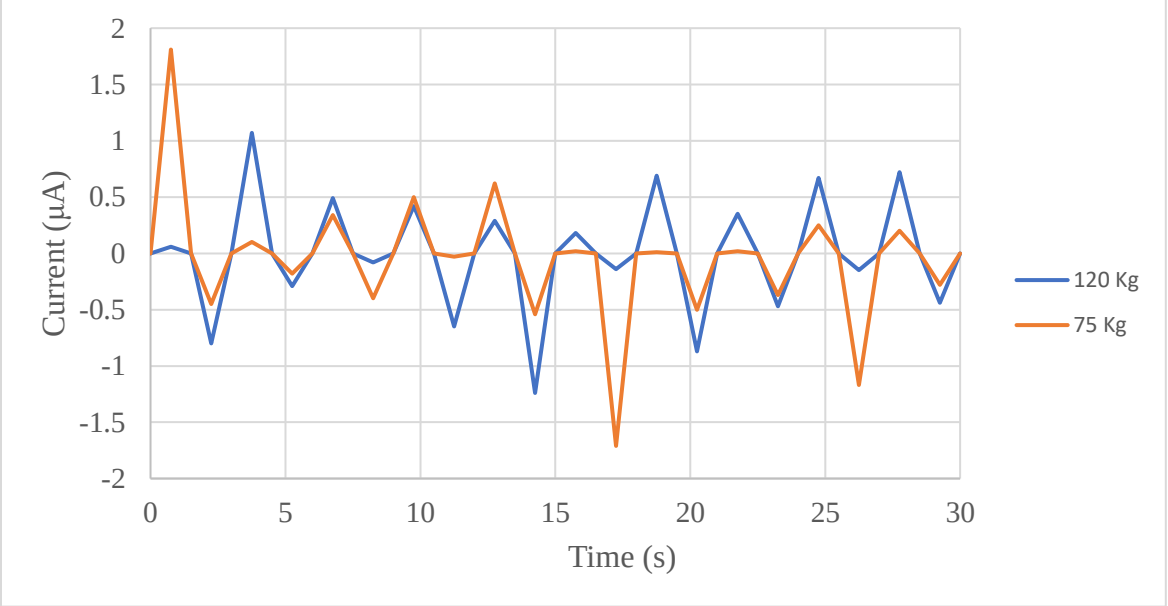

Fig. 12 Current (in µA) in the third setup.

The results of this experiment were very counterintuitive, as when both setups 1 and 2 were tested, both the open circuit voltage and the short circuit current were higher when the TENG was activated under a 750 N weight compared to the 1200 N, which is opposite to what was discussed in the introduction. In setup 3, both the open circuit voltage and short circuit current results were almost equal under both weights. This could be explained by the fact that under a higher weight, the sponges take a longer time to return to their original shape, and since the distance between the two sides of the TENG is directly proportional to the output voltage, [19], the output voltage would be slightly lower in the case of the higher weight.

Another observation that can be made from those results is the fact that the highest values of short circuit current occurred in setup 2. That was also unexpected, as it was hypothesized that a higher surface area would lead to a higher short circuit current. That suggests that the actual contact area in setup 2 was higher than the actual contact area in setup 3. A third significant observation is the very low voltage and current generated in setup 1, compared to both setup 2 and setup 3. This is despite the fact that an equal amount of voltage in all 3 setups should be expected, as the surface area has no effect on the open circuit voltage. These two observations have a potential explanation based on the stability of each setup. Setup 1 is unstable and causes force inequality in the system that leads to the decrease of the actual contact surface area between the Kapton and PMMA. Then the charge density decreases the voltage and current generated, as shown in Fig. 7.

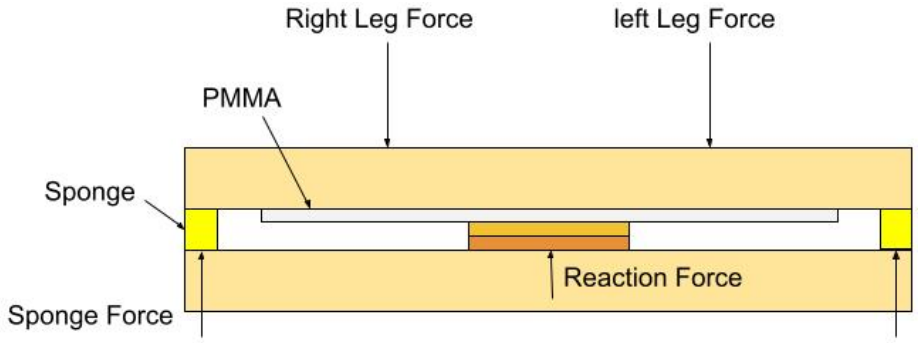

Fig. 7 Forces acting in setup 1.

Setup 2 is stable, as the two reaction forces provide a correcting effect that causes better contact between the Kapton and the PMMA, as shown in Fig. 8.

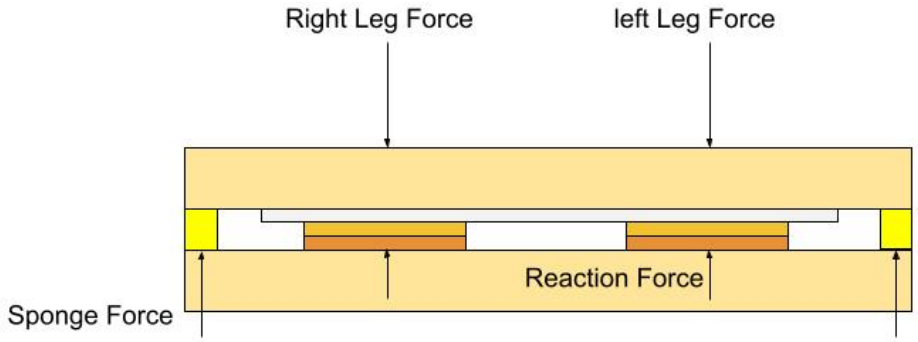

Fig. 8 Forces acting in setup 2.

Setup 3 is slightly less stable than setup 2, it has a large footprint that also helps in self-correction in case of any force inequality. However, if the middle structure is slightly higher than the side structures, the stability of the setup decreases and the actual contact surface area decreases, this is hypothesized to be what happened in the experiment, as shown in Fig. 9.

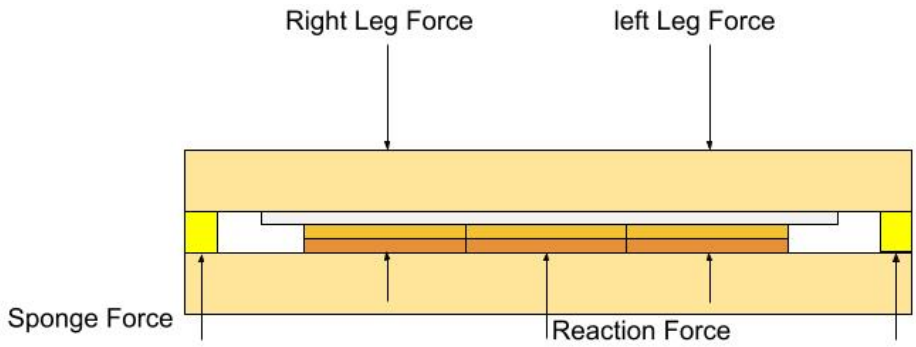

Fig. 9 Forces in setup 3.

CONCLUSIONS

1. The standard of covering the negative side of a TENG with one Kapton terminal is not the most efficient way to design the negative sign of the TENG.
2. Using two different terminals which are spaced apart is the most efficient way to design the Kapton side in a Kapton/PMMA TENG when it comes to obtaining the highest values of both open-circuit voltage and short circuit currents in this experiment.
3. Kapton side should have enough large surface area and a self-correcting mechanism that ensure optimal contact between the two TENG sides.

REFERENCES

1. Al-Qaham, Y., Mohamed M. K., and Ali. W. Y., "Electric Static Charge Generated From the Friction of Textiles", Journal of the Egyptian Society of Tribology, EGTRIB, Vol. 10, No. 2, pp. 45 - 56, (2013).
2. Shivangi N., Mukherjee R., and Chaudhuri B., "Triboelectrification: A review of experimental and mechanistic modeling approaches with a special focus on pharmaceutical powders", International journal of pharmaceutics Vol. 510, No. 1, pp. 375-385, (2016).
3. Ali A. S., "Triboelectrification of Synthetic Strings", Journal of the Egyptian Society of Tribology, EGTRIB, Vol. 16, No. 2, pp. 26-36, (2019).
4. Pan S. and Zhang Z., "Fundamental theories and basic principles of triboelectric effect: a review." Friction, Vol. 7, No. 1, pp. 2-17, (2019).
5. McCarty, Logan S., and George M. Whitesides., "Electrostatic charging due to separation of ions at interfaces: contact electrification of ionic electrets." Angewandte Chemie International Edition, Vol. 47, No. 12, pp. 2188-2207, (2008).
6. Zou H., Zhang Y., Guo L., Wang P., He X., Dai G., Zheng H., Chen C., Wang A. C., Xu C. and Wang Z. L., "Quantifying the triboelectric series", Nature communications, Vol. 10, No. 1, pp. 1427, (2019).
7. Diaz, A. F., and Felix-Navarro R. M., "A semi-quantitative tribo-electric series for polymeric materials: the influence of chemical structure and properties", Journal of Electrostatics, Vol. 62, No. 4, pp. 277-290, (2004).
8. Burgo, Thiago AL, Galembeck F., and Pollack G. H., "Where is water in the triboelectric series?", Journal of Electrostatics Vol. 80, pp. 30 - 33, (2016).
9. Zhang R. and Olin H., "Material choices for triboelectric nanogenerators: a critical review." EcoMat, Vol. 2, No. 4, pp. 120 - 132, (2020).

10. Al-Kabbany A. M., and Ali W. Y., "Reducing the electrostatic charge of polyester by blending by polyamide strings.", Journal of the Egyptian Society of Tribology, Vol. 16, No. 4, pp. 36-44, (2019).
11. Yang Y., Zhu G., Zhang H., Chen J., Zhong X., Lin Z. H., Su Y., Bai P., Wen X. and Wang Z. L., "Triboelectric nanogenerator for harvesting wind energy and as self-powered wind vector sensor system.", ACS nano, Vol. 7, No. 10, pp. 9461-9468, (2013).
12. Zhang H., Yang Y., Su Y., Chen J., Adams K., Lee S., Hu C. and Wang, Z. L., "Triboelectric nanogenerator for harvesting vibration energy in full space and as self-powered acceleration sensor.", Advanced Functional Materials, Vol. 24, No. 10, pp. 1401-1407, (2014) .
13. Cheng P., Guo H., Wen Z., Zhang C., Yin X., Li X., Liu D., Song W., Sun X., Wang J. and Wang Z. L., "Largely enhanced triboelectric nanogenerator for efficient harvesting of water wave energy by soft contacted structure.", Nano Energy, Vol. 57, pp. 432-439, (2019).
14. Wang X., Niu S., Yin Y., Yi F., You Z. and Wang Z. L., "Triboelectric nanogenerator based on fully enclosed rolling spherical structure for harvesting low-frequency water wave energy.", Advanced Energy Materials, Vol. 5, No. 24, 1501467, (2015).
15. Jin T., Sun Z., Li L., Zhang Q., Zhu M., Zhang Z., Yuan G., Chen T., Tian Y., Hou X. and Lee C., "Triboelectric nanogenerator sensors for soft robotics aiming at digital twin applications.", Nature communications, Vol. 11, No .1, pp, 1-12, (2020).
16. Qin K., Chen C., Pu X., Tang Q., He W., Liu Y., Zeng Q., Liu G., Guo H. and Hu C., "Magnetic array assisted triboelectric nanogenerator sensor for real-time gesture interaction.", Nano-micro letters, Vol. 13, No. 1, .pp. 1-9, (2021).
17. Zhou Q., Pan J., Deng S., Xia F. and Kim T., "Triboelectric Nanogenerator-Based Sensor Systems for Chemical or Biological Detection.", Advanced Materials, Vol. 33, No. 35, 2008276, (2021).
18. Dhakar L., Pitchappa P., Tay F. E. H. and Lee C., "An intelligent skin based self-powered finger motion sensor integrated with triboelectric nanogenerator.", Nano Energy, Vol. 19, pp, 532-540, (2016).
19. Niu S., Wang S., Lin L., Liu Y., Zhou Y. S., Hu Y. and Wang Z. L., "Theoretical study of contact-mode triboelectric nanogenerators as an effective power source.", Energy & Environmental Science, Vol. 6, No. 12, pp. 3576-3583, (2013).
20. Dharmasena R. D. I. G., Jayawardena K. D. G. I., Mills C.A., Dorey R. A. and Silva S. R. P., "A unified theoretical model for Triboelectric Nanogenerators.", Nano Energy, Vol. 48, pp. 391-400, (2018).
21. Xu Y., Min G., Gadegaard N., Dahiya R. and Mulvihill D. M., "A unified contact force-dependent model for triboelectric nanogenerators accounting for surface roughness.", Nano Energy, Vol. 76, 105067, (2020).
22. Zhu G., Lin Z. H., Jing Q., Bai P., Pan C., Yang Y., Zhou Y. and Wang Z. L., "Toward large-scale energy harvesting by a nanoparticle-enhanced triboelectric nanogenerator.", Nano letters, Vol. 13, No. 2, pp. 847-853, (2013).
23. Chen J., Zhu G., Yang W., Jing Q., Bai P., Yang Y., Hou T. C. and Wang Z. L., "Harmonic-resonator-based triboelectric nanogenerator as a sustainable power source and a self-powered active vibration sensor." Advanced materials, Vol. 25, No. 42, pp. 6094-6099, (2013).

24. Wang S., Lin L., Xie Y., Jing Q., Niu S. and Wang Z. L., "Sliding-triboelectric nanogenerators based on in-plane charge-separation mechanism.", Nano letters, Vol. 13, No. 5, pp. 2226-2233, (2013).
25. Lin L., Wang S., Xie Y., Jing Q., Niu S., Hu Y. and Wang Z. L., "Segmentally structured disk triboelectric nanogenerator for harvesting rotational mechanical energy.", Nano letters, Vol. 13, No. 6, pp. 2916-2923, (2013).